# Drag reduction in a Turbulent Channel Flow
# by Using a GA-based Feedback Control System

Yuji SUZUKI, Takashi YOSHINO, Tsuyoshi YAMAGAMI and Nobuhide KASAGI

Department of Mechanical Engineering, The University of Tokyo,

Hongo 7-3-1, Bunkyo-ku, Tokyo, 113-8656, Japan.

e-mail: ysuzuki@thtlab.t.u-tokyo.ac.jp

A prototype system for feedback control of wall turbulence is developed, and its performance is evaluated in a physical experiment. Arrayed micro hot-film sensors with a spanwise spacing of 1 mm are employed for the measurement of the streamwise shear stress fluctuations, while arrayed magnetic actuators having 3 mm in spanwise width are used to introduce control input through wall deformation. A digital signal processor having a time delay of 0.1 ms is employed to drive output voltage for the actuators. Feedback control experiments are made in a turbulent air channel flow. Noise-tolerant genetic algorithm is employed to optimize control parameters. It is found that the wall shear stress is decreased by up to 7% in physical experiments for the first time. Reynolds shear stress close to the wall is decreased by the present control scheme. By using conditional sampling of DNS database, we found that wall induces wall-normal velocity away from the wall, when high-speed regions are located above the actuator.

## 1. INTRODUCTION

In the last decade, feedback control of wall turbulence has been extensively pursued, because its high efficiency is reported in various studies using direct numerical simulation (DNS)[1-3]. In order to realize such a control system, coherent structures such as the near-wall streamwise vortices, which are responsible for regeneration cycle of turbulence and wall skin friction, should be detected by wall sensors, and selectively manipulated by the motion of actuators mounted on the wall. Although the coherent structures have generally very small spatio-temporal scales, recent development of microelectromechanical systems (MEMS) technology has made it possible to fabricate flow sensors and mechanical actuators of submillimeter scale[4].

Endo et al.[5] carried out a DNS of turbulent channel flow, in which arrayed wall shear stress sensors and wall-deformation actuators of finite spatial dimensions are assumed. They obtained drag reduction of 12% by attenuating the near-wall streamwise vortices. Morimoto et al.[6] assumed the streamwise wall shear stress fluctuation as the sensor information, and developed a feedback control scheme based on genetic algorithms (GA) with the aid of DNS. These findings encourage us to develop a feedback control system as shown in Fig. 1; the control system consists of rows of micro wall-shear stress sensors and wall-deformation actuators. In 5th Symposium on Smart Control of Turbulence, we reported reduction in the wall-shear stress fluctuations using our first prototype[7].

The objectives of the present study are to develop a prototype of feedback control system with arrayed micro hot-film shear stress sensors and wall-deformation magnetic actuators, and to evaluate its performance of drag reduction in a turbulent channel flow.

## 2. FEEDBACK CONTROL SYSTEM WITH GA-BASED ALGORITHMS

Figure 2a shows our 2nd generation control system. It has four sensor rows and three actuators rows in between. Each sensor row has 48 micro wall-shear stress sensors with 1mm spacing, and each actuator row has 16 wall-deformation actuators with 3mm spacing. Magnified view and schematic of the cross section of the shear stress sensor is shown in Fig. 2b. A platinum hot-film is deposited on a $SiN_X$ diaphragm ($400{\times}400\mu m^2$) of 1 μm in thickness, and a 200 μm-deep air cavity is formed underneath. We found that the frequency response of this first generation sensor is somewhat low, and the gain is deteriorated at $f>170Hz$[8]. However, it is also found that the spanwise two-point correlation of $\tau'_w$ measured with the arrayed sensors is in good accordance with the DNS data[9]. Therefore, the near-wall coherent structures, which are the target of the feedback control, can be well captured with the present wall shear stress sensors.

For the wall-deformation magnetic actuator, a silicone rubber sheet of 0.1mm in thickness is used as an elastic membrane having dimensions of 2.4mm and 14mm respectively in the spanwise and streamwise directions. A rare-earth miniature permanent magnet and a miniature copper coil elongated in the streamwise direction are used (Fig. 2c). The resonant frequency is 800Hz for 10 $Vp\text{-}p$ signal with a maximum amplitude of about 50μm.

A digital signal processor (DSP) system (MPC7410, MTT Inc.) with 224 analog input and 96 output channels is used as the controller of the present system. The output voltage of the constant temperature circuits for the hot-film sensors are digitized with 14bit AD converters. The control signals for the actuators are then computed with the DSP, and converted back to analog signals using 14bit DA converters. The processing time in the DSP is within 0.1ms, and the repetition frequency of the control loop is 5kHz, which is believed to be sufficiently high if compared with the characteristic time scale of the turbulence.

A turbulent air channel flow facility is employed for evaluating the present feedback control system. The cross section of the channel is $50{\times}500mm^2$, and the test section is located 4m downstream from the inlet, where the flow is fully-developed. The control system is placed at the bottom wall of the test section as shown in Fig. 3a. The bulk mean velocity $U_m$ is set to be 3m/s, which corresponds to the Reynolds number $Re_\tau$ based on the wall friction velocity $u_\tau$ and the channel half-width of 300. Under the present flow condition, one viscous length and time unit correspond to 0.09mm and 0.5ms, respectively. Thus, the mean diameter of the near-wall streamwise vortices is estimated to be 2.7mm, and its characteristic time scale is 7.5ms. The flow field is measured with a three-beam two-component LDV system (DANTEC, 60X51) as shown in Fig. 3b. The measurement volume is about ϕ160μmx3.5mm.

An optimal control scheme based on genetic algorithm (GA)[6] is employed in the present experiment. Driving voltage of each wall-deformation actuator $E_A$ is determined with a linear combination of the streamwise wall shear stress fluctuations $\tau_w'_i$, i.e.,

$$E_A = \sum_{i=1,3} W_i \tau'_{w,i} \tag{1}$$

where $\tau_w'_i$ is measured with three sensors located upstream as shown in Fig. 4. The spacing between neighboring sensor used in the present control scheme is 36 viscous units. Note that actuators move upwards when $E_A$ is positive, while downwards when negative. The control variables $W_i$ are optimized in such a way that the mean wall shear stress measured with three sensors at the most downstream location is minimized. The cost function $J$, which equals the drag reduction rate, is then defined by

$$J = 1 - \frac{\sum\limits_{j=1,3}\left(\int_0^T \tau_{w,j}\,dt\right)}{\sum\limits_{j=1,3}\left(\int_0^T \tau_{w,j}\big|_{no-control}\,dt\right)},$$ (2)

and $J$ is maximized. Each $W_i$ is expressed with a binary-coded string with 5 bits, which corresponds to a gene, and $N$ individuals including a set of genes are made. Feedback control experiment using each individual, i.e., different set of $W_i$s is independently carried out, and the cost function is calculated on line. Then, individuals having smaller cost are statistically selected as parents, and offsprings are made through crossover operation. Finally, mutation at a given rate is applied to all genes of the $N$ individuals. Elite selection strategy is also adopted, so that gene having maximum cost is preserved. New generations are successively produced by repeating this procedure. The integration time $\Delta T$ is chosen as 20s ($\Delta T^+=4000$).

We found in our preliminary experiment that the mean wall shear stress integrated over $\Delta T$ has still relatively-large random error of about 3%, although $\Delta T$ is much longer than the characteristic time scale of the turbulent flow field. This is partially due to the small temporal variation of air temperature, which is inevitable in the present experiment lasting for more than ten hours. Therefore, we employed a noise-tolerant GA method, in which genes with random numbers are introduced at each generation[10]. The population size $N$ and number of generation are respectively chosen as 10 and 100. Thus, in total, 1000 trials with different set of control variables are made out of $2^{15}=32768$ possible combination of genes.

## 3. CONTROL EXPERIMENTS IN TURBULENT CHANNEL FLOW

Figure 5a shows the evolution of the cost function. The data are scattered in a wide range because of the genes with random number introduced, but we have obtained $7\pm3\%$ drag reduction if we consider 3% error in $J$. Figure 5b shows the distribution of optimum $W_i$, which corresponds to the optimum gene obtained. It is found that $W_i$s are all negative, and about half of the genes tested in the present experiment have a similar trend. Therefore, it is clear that drag reduction is achieved with negative $W_i$s in the present experiment. It is also noted that, when all $W_i$s is kept positive without using the GA algorithms, no drag reduction is obtained (not shown).

Figures 6-8 show profiles of the mean velocity, the rms values of velocity fluctuations and the Reynolds shear stress above the center of a actuator measured with LDV. Turbulent statistics obtained for unmanipulated flow are in good agreement with the DNS data[9]. When the present feedback control is applied, the mean velocity profile and the rms values are unchanged. However, the Reynolds shear stress close to the wall is decreased. Fukagata et al.[11] showed that the reduction in the Reynolds stress near the wall has a direct contribution to the drag reduction. Therefore, the drag reduction is also confirmed through the present LDV measurement.

## 4. IMPLICATION OF THE PRESENT CONTROL SCHEME

Since optimum $W_i$s are negative, actuators move downward when $\tau_w$' is positive. However, it is not straightforward to interpret the effect of the present control scheme on the near-wall coherent structures. Thus, we made a conditional average of a DNS database[9,12] in order to examine the flow structure near the actuators. Since the wall deformation is much smaller than the thickness of the viscous sublayer, the deformed shape itself has little effect on the flow field. Instead, the flow velocity induced by the wall motion can modify the flow field[5]. Therefore, we define $q$ as the time derivative of $E_A$,

$$q \equiv \frac{dE_A}{dt} = \frac{d}{dt}\left(\sum_{i=1,3} W_i \tau'_{w,i}\right), \tag{3}$$

and use $q$ as the indicator of the wall velocity. Strictly speaking, the wall velocity is not proportional to $q$ due to the nonlinear response of the actuator, but we believe that conditionally-averaged field based on large $q$ should associated with large wall velocity.

Figure 9 shows a 3-D structure associated with $q>q_{rms}$ corresponding to the upward motion of the wall. Low- and high-speed regions are respectively observed upstream and downstream the detection point, and internal shear layer is formed at the interface. This is because, positive $q$ also corresponds to negative $d\tau_w/dt$, corresponding the deceleration at the detection point. Figure 10 shows velocity vectors and contours of the streamwise velocity fluctuations in a cross-stream plane located at 100 viscous units downstream the detection point, where the center of the actuator is located. It is found that a high-speed region is located near the wall, and the wall-normal velocity near the buffer layer is negative. There, when $q>q_{rms}$, the present control scheme induces the wall velocity 180 degree out-of-phase with the fluid velocity above actuators.

Although it is not shown here, the conditional sampling for $q<-q_{rms}$ is also made, which corresponds to acceleration at the detection point and to the downward motion of the wall. It is found that the conditional-averaged structure is somewhat smeared out, and the wall-normal velocity near the buffer layer is slightly negative, which is in-phase with the motion of the actuator. Therefore, the actuator motion with the present scheme should be only similar with v-control[13] for positive $q$, but not exactly the same. Further analysis is necessary for more detailed control mechanism.

## 5. THIRD GENERATION CONTROL SYSTEM

Figure 11 shows our 3rd-generation control system. The hot-film wall shear stress sensor is designed based on detailed thermal analysis to improve its frequency response, and a novel feed-through technique is employed to realize backside electronic connection. As described in [7], we confirmed that the power spectrum of the wall shear stress fluctuation is in good agreement with DNS data at $Re_\tau \sim 650$, and its cut-off frequency is about up to 520Hz, where the measured power spectrum is 50% of the DNS data.

The outlook of the actuator array is almost the same as the second generation. However, the present actuator is designed to reduce power consumption and to improve magnetic cross talk between neighboring actuators. For those purposes, we employ Permalloy for magnetic shield and core of the coil, and their geometry is optimized with FEM analysis of the magnetic field[7]. The resonant frequency is about 700Hz.

The system consists of 8 rows of sensors and 7 rows of actuators. In total, 288 micro sensors and 84 actuators are integrated. Driving circuit boards for the sensors and the actuators are also developed. Fast DSP used in our 2nd-generation system is also employed. Due to the larger control area, we expect that the 3rd generation system offers larger drag reduction than the 2nd generation. Currently, all the system is assembled, and the initial test is undertaken in the turbulent channel flow.

## CONCLUSIONS

The prototype of the feedback control system for wall turbulence is developed using arrayed micro hot-film sensors and arrayed magnetic wall-deformation actuators. Driving voltage of the actuators is

assumed to be a linear combination of the wall shear stress fluctuations measured at three locations upstream, and the weights are optimized by using a noise-tolerant genetic algorithm in such a way that the time integral of the wall shear stress is minimized. We have obtained about 7% skin friction reduction in a turbulent channel flow for the first time. The Reynolds shear stress is also found to be decreased near the wall. We also found in conditional sampling of a DNS database that, with the present control scheme, the wall-deformation actuators move upwards beneath the near-wall high-speed regions.

**REFERENCES**

[1] Moin, P., and Bewley, T., Appl. Mech. Rev., Vol. 47, (1994), pp. S3-S13.

[2] Gad-el-hak, M., Appl. Mech. Rev., Vol. 49, (1996), pp. 365-379.

[3] Kasagi, N., Int. J. Heat & Fluid Flow, Vol. 19, (1998), pp. 128-134.

[4] Ho, C.-M., and Tai, Y.-C., ASME J. Fluids Eng. Vol. 118, (1996), pp. 437-447.

[5] Endo, T., Kasagi, N., and Suzuki, Y., Int. J. Heat & Fluid Flow, Vol. 21, (2000), pp. 568-575.

[6] Morimoto, S., Iwamoto, K., Suzuki, Y., and Kasagi, N., Bull. Am. Phys. Soc., Vol. 46, (2001), p. 185.

[7] Park, J., Yoshino, T., Suzuki, Y., and Kasagi, N., Proc. 5th Symp. on Smart Control of Turbulence, Tokyo, (2004), pp. 111-117.

[8] Yoshino, T., Suzuki, Y., Kasagi, N., and Kamiunten, S., Proc. IEEE Int. Conf. MEMS 2003, Kyoto, (2003), pp. 193-196.

[9] Iwamoto, K., Suzuki, Y., and Kasagi, N., Int. J. Heat & Fluid Flow, Vol. 23, (2002), pp. 678-689.

[10] Tobita, T., Fujino, A., Segawa, K., Yoneda, K., and Ichikawa, Y., Electrical Engineering in Japan, Vol. 124, (1998), pp. 55-64.

[11] Fukagawa, K., Iwamoto, K., and Kasagi, N., Phys. Fluids, Vol. 14, (2002), pp. L73-L76.

[12] Iwamoto, K., (2005), private communication.

[13] Choi, H., Moin, P., and Kim, J., J. Fluid Mech., Vol. 262, (1994), pp. 75-110.
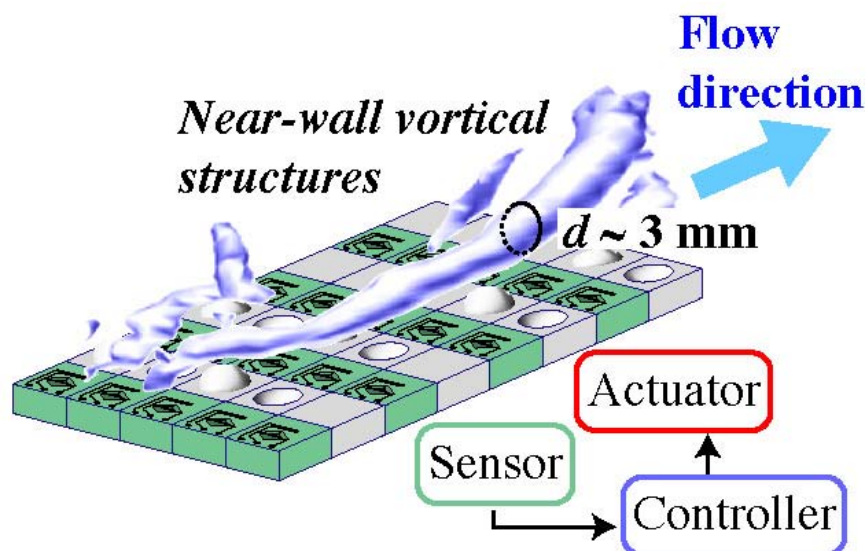


Figure 1 Schematic diagram of active feedback control system for wall turbulence.
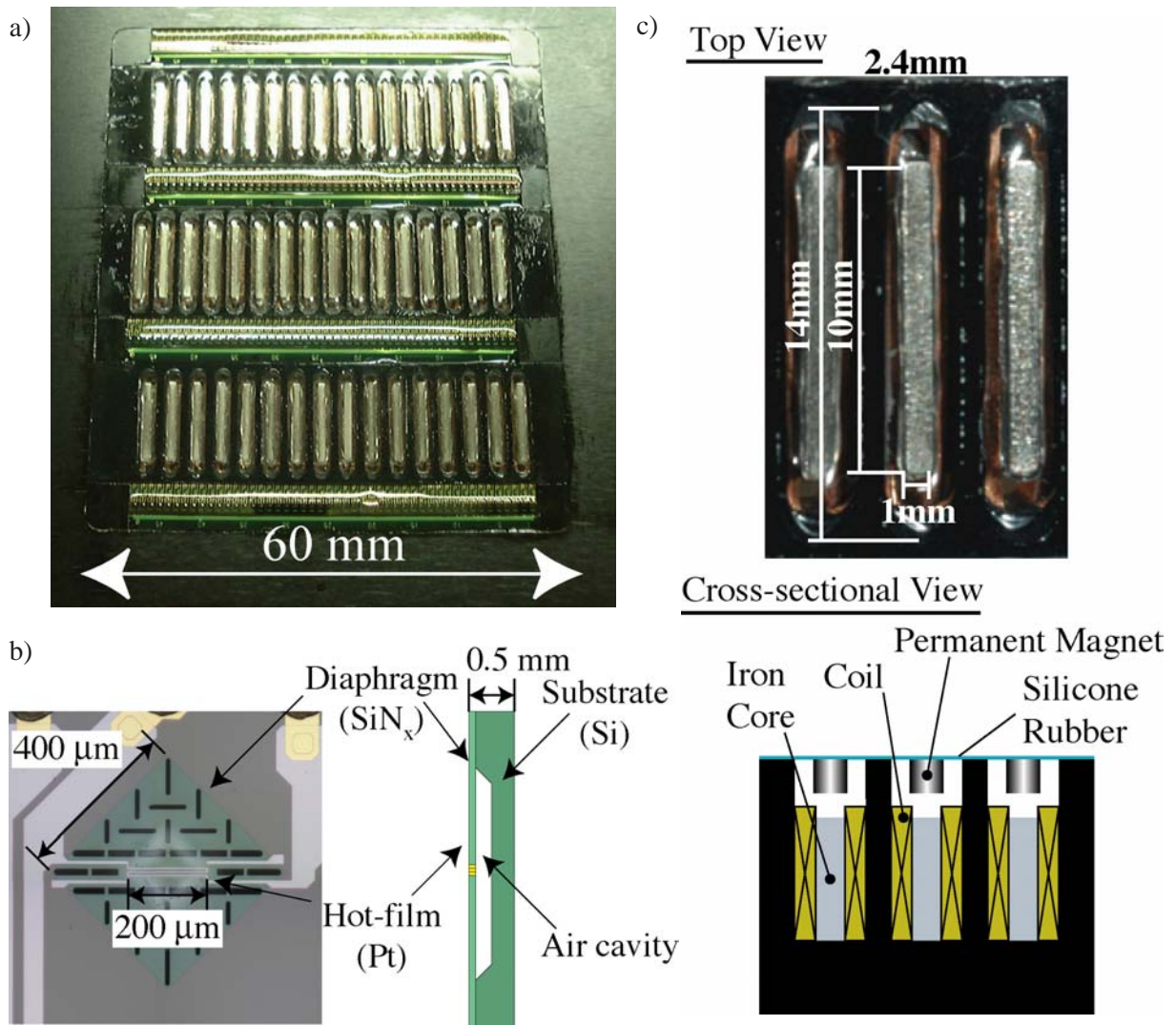
Figure 2 Second-generation feedback control system for wall turbulence. a)Plane view of the system having 192 wall shear stress sensors and 48 wall-deformation actuators, b)Magnified view of a sensor, c)Magnified view of actuators.
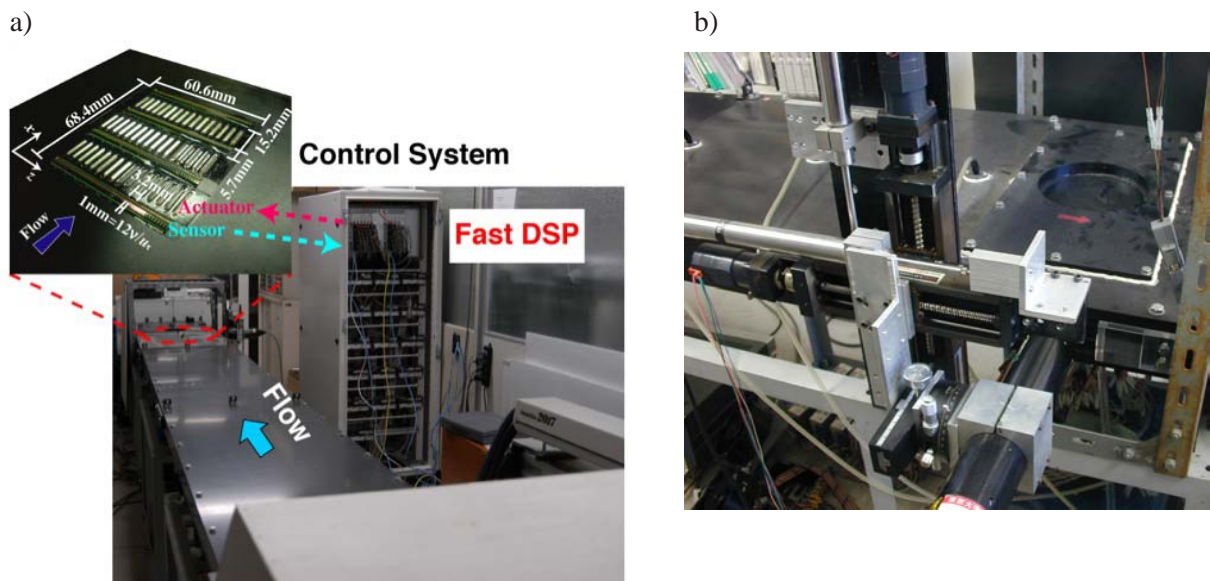


Figure 3 Experimental setup. a)Turbulent air channel flow facility and DSP control system, b)Test section and LDV traversing mechanism.
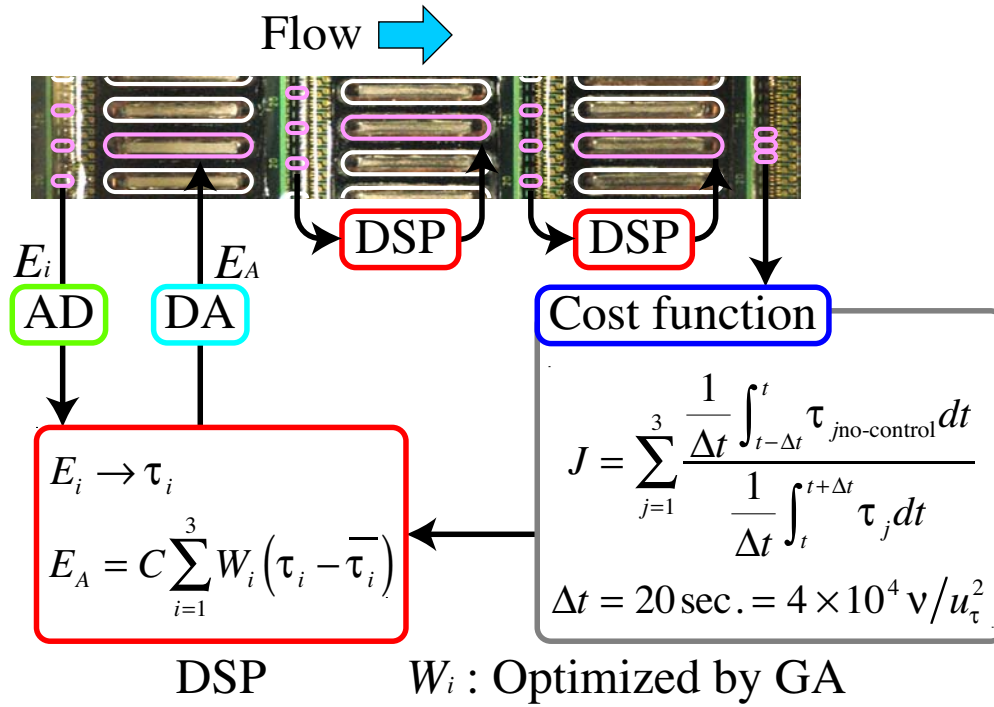
Flow ⟶

$E_i$
AD

$E_A$
DA

DSP    DSP

Cost function

$E_i \rightarrow \tau_i$

$E_A = C \sum_{i=1}^{3} W_i \left( \tau_i - \overline{\tau_i} \right)$

DSP

$$J = \sum_{j=1}^{3} \frac{\frac{1}{\Delta t} \int_{t-\Delta t}^{t} \tau_{j\text{no-control}} dt}{\frac{1}{\Delta t} \int_{t}^{t+\Delta t} \tau_j dt}$$

$\Delta t = 20\,\text{sec.} = 4 \times 10^4 \, \nu / u_\tau^2$

$W_i$ : Optimized by GA

Figure 4 Result of GA-based feedback control in a turbulent channel flow. a)Cost function versus generation, b)Optimum weight.

a)


b)
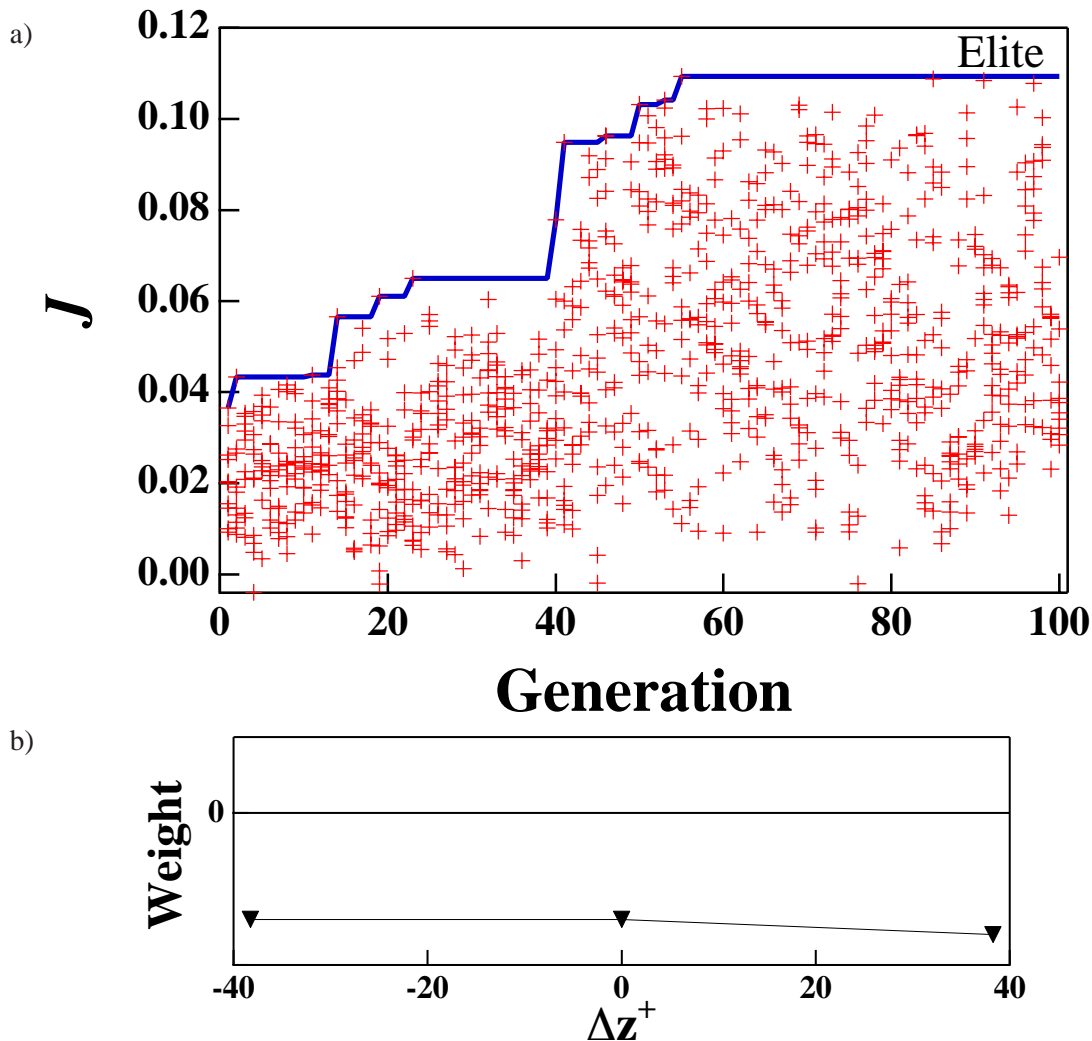

Figure 5 Result of GA-based feedback control in a turbulent channel flow. a)Cost function versus generation, b)Optimum weight.
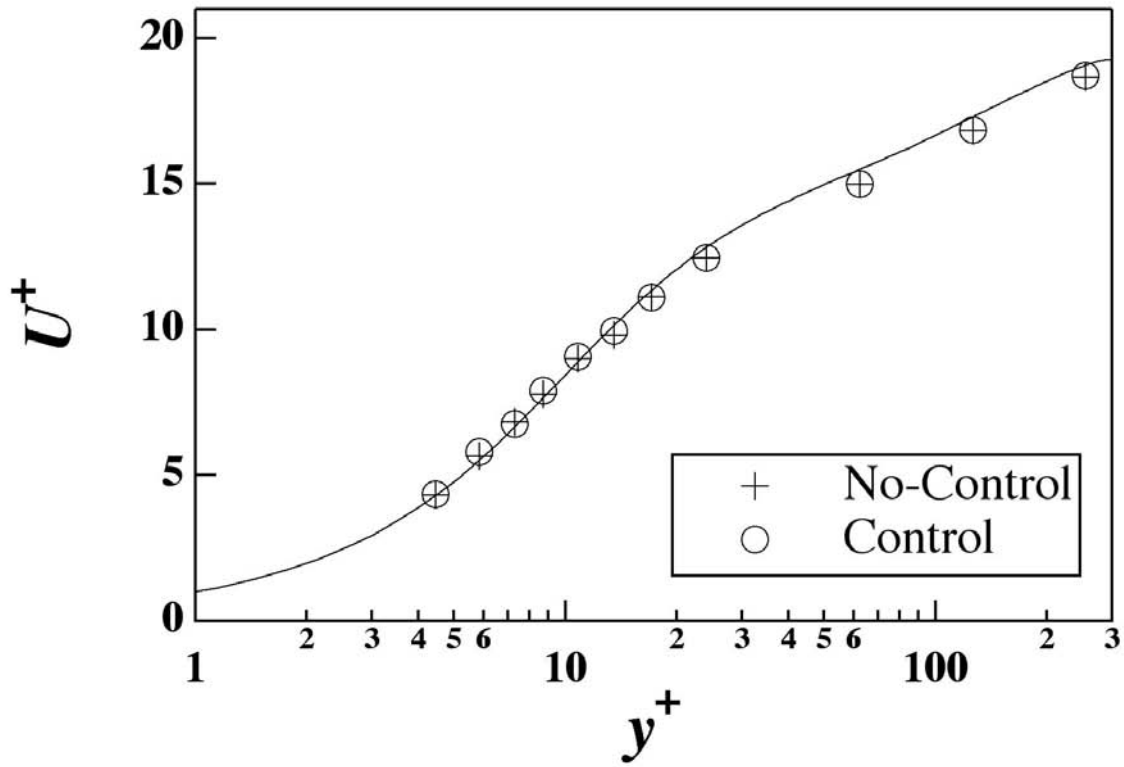
Figure 5 Mean velocity profile above the center of actuator. The wall friction velocity is estimated for unmanipulated flow.
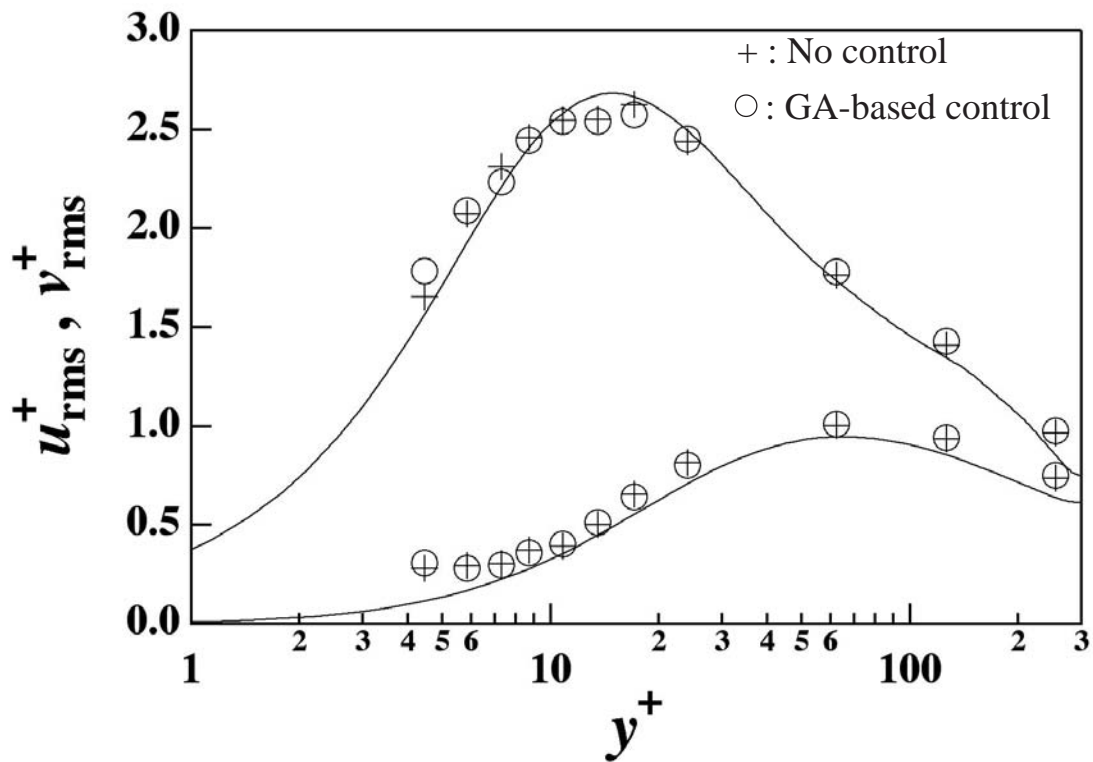


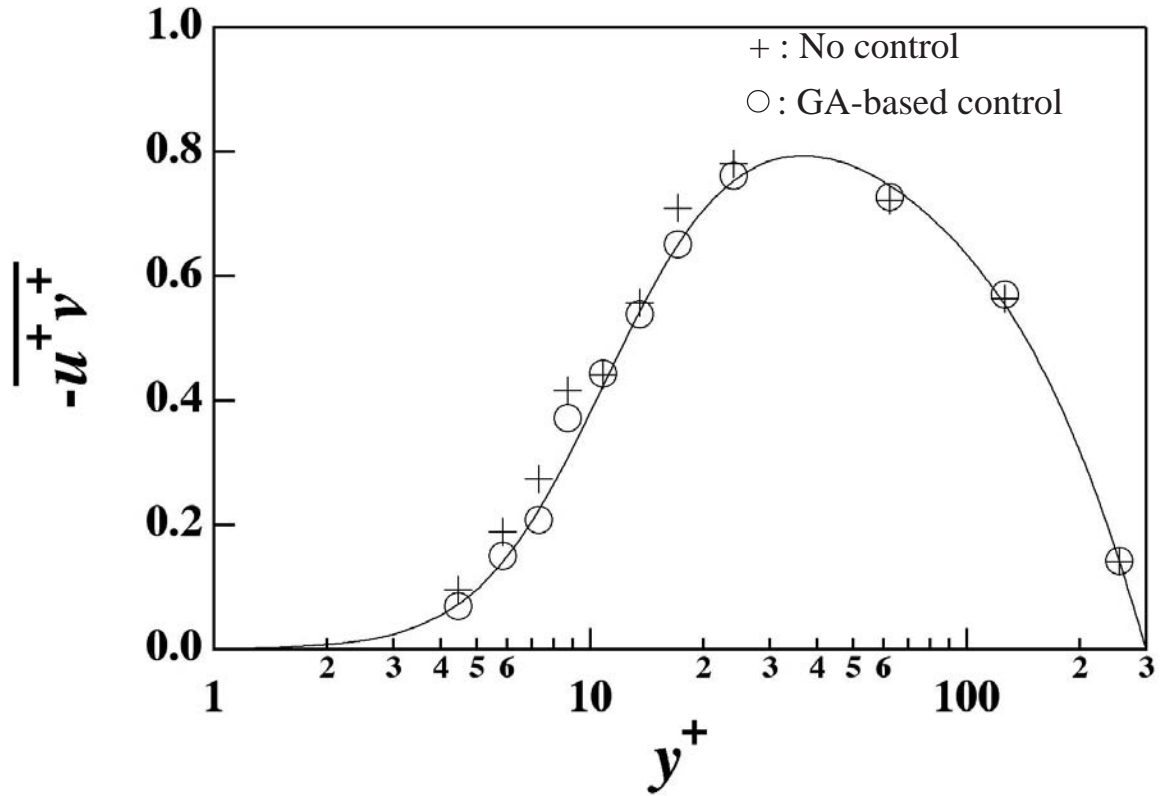Figure 6 Distribution of rms values of velocity fluctuations above the center of actuator.

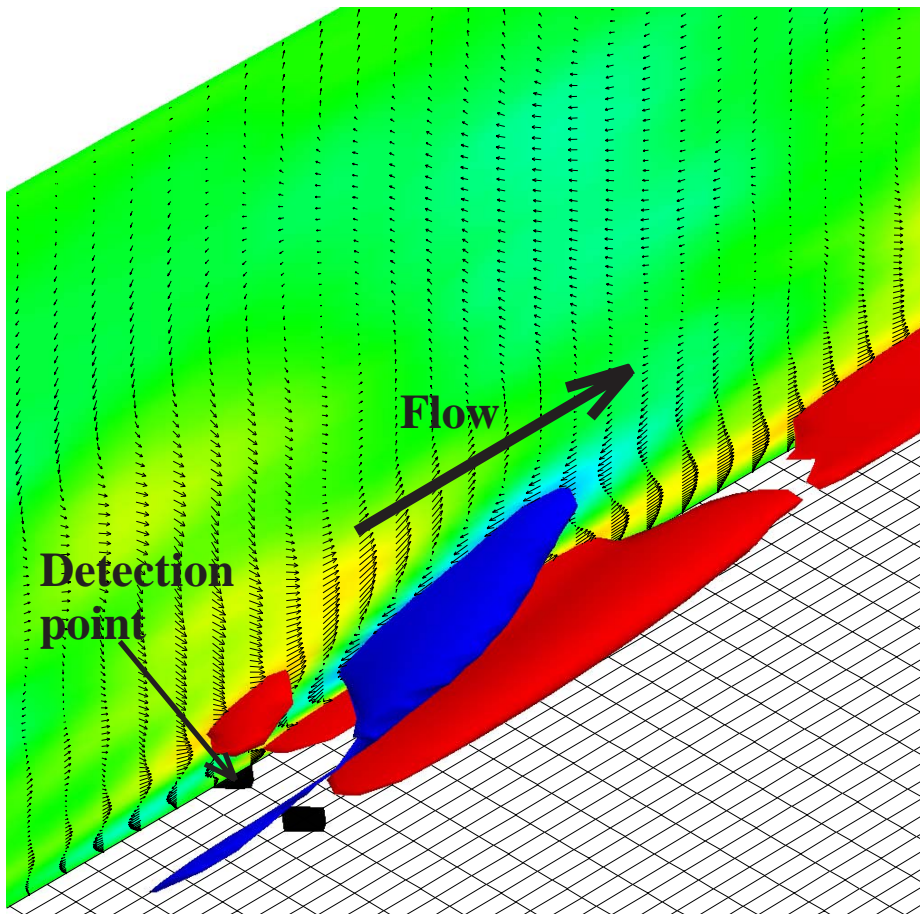Figure 8 Reynolds shear stress distribution above the center of actuator.



Figure 9 Conditional-averaged 3D velocity field associated with events $q > q_{rms}$. Blue to red, $<u^+> = -0.5$ to $0.5$.
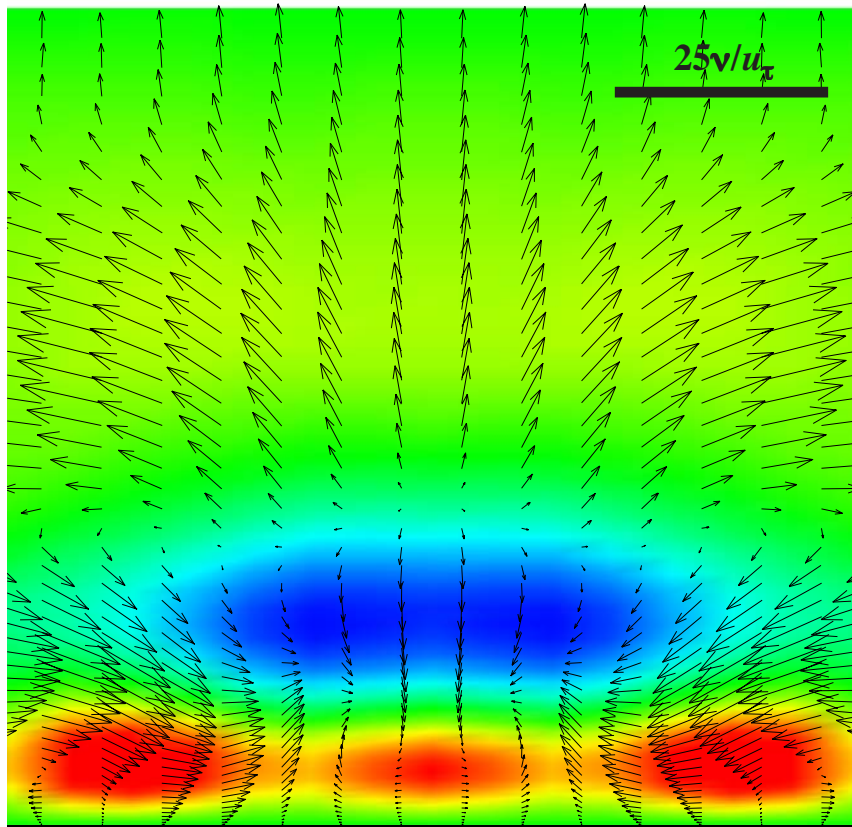
Figure 10 Conditional-averaged velocity field in the *y-z* plane at $x^+=100$ associated with events $q>q_{rms}$.  Blue to red, $<u^+> = $ -0.5 to 0.5.
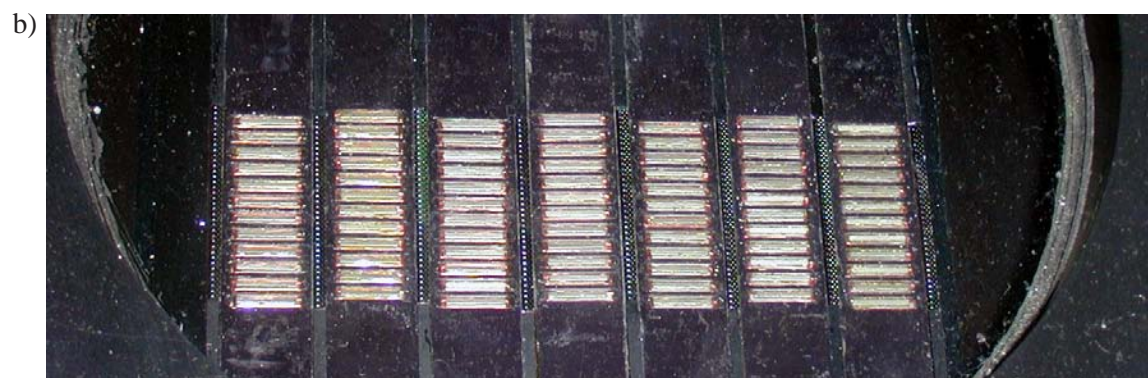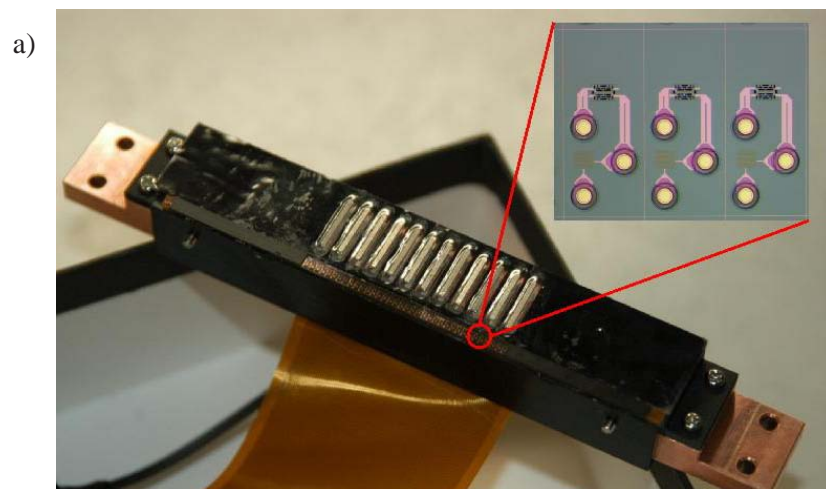
a)



b)



Figure 11 3rd-generation control system having 288 wall-shear stress sensors, 84 wall-deformation actuators.  a)Photo of a sensor raw and an actuator raw , b)Integrated system installed in the channel.